Journal of Cerebral Blood Flow & Metabolism (2011) 31, 1778–1787

www.jcbfm.com

Stroke penumbra defined by an MRI-based oxygen challenge technique: 1. Validation using [^{14}C]2-deoxyglucose autoradiography

Craig A Robertson[1], Christopher McCabe[1], Lindsay Gallagher[1], Maria del Rosario Lopez-Gonzalez[2], William M Holmes[1], Barrie Condon[3], Keith W Muir[4], Celestine Santosh[3] and I Mhairi Macrae[1]

[1]*Glasgow Experimental MRI Centre, Institute of Neuroscience and Psychology, College of Medical, Veterinary and Life Sciences, University of Glasgow, Glasgow, UK;* [2]*Department of Clinical Physics, SINAPSE Collaboration, College of Medical, Veterinary and Life Sciences, University of Glasgow, Glasgow, UK;* [3]*Institute of Neurological Sciences, Southern General Hospital, Glasgow, UK;* [4]*Institute of Neuroscience and Psychology, University of Glasgow, Institute of Neurological Sciences, Southern General Hospital, Glasgow, UK*

Accurate identification of ischemic penumbra will improve stroke patient selection for reperfusion therapies and clinical trials. Current magnetic resonance imaging (MRI) techniques have limitations and lack validation. Oxygen challenge T_2^* MRI (T_2^* OC) uses oxygen as a biotracer to detect tissue metabolism, with penumbra displaying the greatest T_2^* signal change during OC. [^{14}C]2-deoxyglucose (2-DG) autoradiography was combined with T_2^* OC to determine metabolic status of T_2^*-defined penumbra. Permanent middle cerebral artery occlusion was induced in anesthetized male Sprague-Dawley rats ($n = 6$). Ischemic injury and perfusion deficit were determined by diffusion- and perfusion-weighted imaging, respectively. At 147 ± 32 minutes after stroke, T_2^* signal change was measured during a 5-minute 100% OC, immediately followed by 125 μCi/kg 2-DG, intravenously. Magnetic resonance images were coregistered with the corresponding autoradiograms. Regions of interest were located within ischemic core, T_2^*-defined penumbra, equivalent contralateral structures, and a region of hyperglycolysis. A T_2^* signal increase of 9.22% ± 3.9% (mean ± s.d.) was recorded in presumed penumbra, which displayed local cerebral glucose utilization values equivalent to contralateral cortex. T_2^* signal change was negligible in ischemic core, 3.2% ± 0.78% in contralateral regions, and 1.41% ± 0.62% in hyperglycolytic tissue, located outside OC-defined penumbra and within the diffusion abnormality. The results support the utility of OC-MRI to detect viable penumbral tissue following stroke.
Journal of Cerebral Blood Flow & Metabolism (2011) **31,** 1778–1787; doi:10.1038/jcbfm.2011.66; published online 11 May 2011

Keywords: ADC; CBF; imaging; LCMRglu; MCAO; rat

Introduction

Stroke is a leading cause of morbidity and the second most common cause of mortality worldwide (Donnan *et al*, 2008). Disability and mortality are reduced by admission to specialized stroke units, but the only widely approved drug treatment for acute cerebral ischemia is recombinant tissue plasminogen activator, for which many patients are ineligible. Low treatment rates with intravenous recombinant tissue plasminogen activator (e.g., 1% to 7% in the United States following FDA approval; Wardlaw *et al*, 2009) partly reflect delay in presentation and institutional barriers to rapid medical assessment (Katzan *et al*, 2004; Kahn *et al*, 2005), but also that clinical uncertainty prevents treatment in many circumstances. Such clinical uncertainty includes patients

Correspondence: CA Robertson, Wellcome Surgical Institute, Institute of Neuroscience and Psychology, College of Medical, Veterinary and Life Sciences, University of Glasgow, Garscube Estate, Glasgow G61 1QH, UK.
E-mail: c.robertson.1@research.gla.ac.uk
This study was supported by an MRC Project grant (G0700439); the Translational Medicine Research Collaboration (NS-GU-122)—a consortium made up of the Universities of Aberdeen, Dundee, Edinburgh and Glasgow, the four associated NHS Health Boards (Grampian, Tayside, Lothian and Greater Glasgow and Clyde), Scottish Enterprise and Wyeth Pharmaceuticals; an MRC Capacity Building Area PhD studentship 2007 (to CR); and SINAPSE Collaboration funding (to Md RL-G) http://www.sinapse.ac.uk, a Pooling Initiative funded by the Scottish Funding Council and the Chief Scientist Office of the Scottish Executive.
Received 8 November 2010; revised 29 March 2011; accepted 30 March 2011; published online 11 May 2011

awaking with symptoms in whom onset time is unclear, rapidly improving or mild symptoms, and perceived concern about bleeding risks (Barber *et al*, 2001). Failure to identify efficacy in both thrombolysis and neuroprotection trials (Kidwell *et al*, 2001) could have arisen from treatment being administered at a time point when no salvageable (penumbral) tissue remained, but potentially also from recruitment of patients lacking target penumbral tissue even within conventional time windows (Muir, 2002). The possible improvement in safety with more advanced penumbral imaging selection for thrombolysis has also been suggested (Schellinger *et al*, 2003).

MRI-based diffusion-weighted imaging/perfusion-weighted imaging (DWI/PWI) mismatch provides an indirect index of the ischemic penumbra. When used to select patients for thrombolysis, it identified patterns that may define treatment responsiveness (DEFUSE (the diffusion and perfusion imaging evaluation for understanding stroke evolution) study; Albers *et al*, 2006) and has been used to select patients for an extended time window (Hacke *et al*, 2005). However, the technique has not been validated clinically and has a number of limitations. No DWI or apparent diffusion coefficient (ADC) threshold has been determined that can differentiate between irreversibly damaged and potentially recoverable tissue (Guadagno *et al*, 2004) and when thresholds are applied, the lesions identified can be fully or partially reversed by reperfusion in animal models and humans (Kidwell *et al*, 2000). Defining a threshold for the perfusion deficit is equally difficult and may include benign oligemic tissue, which is not at risk (Butcher *et al*, 2005).

We have developed an alternative technique that identifies the penumbra based on its metabolic status, which could represent significant improvements on current penumbral imaging. Oxygen challenge (OC) MRI uses a transient hyperoxic challenge to identify changes in the deoxyhemoglobin:oxyhemoglobin ratio, detected by T_2^*-weighted MRI (Santosh *et al*, 2008; Dani *et al*, 2010). Paramagnetic deoxyhemoglobin and free oxygen in the plasma reduce T_2^* signal, while diamagnetic oxyhemoglobin has a minimal influence on T_2^* (Uematsu *et al*, 2007). Following stroke, penumbral oxidative metabolism ($CMRO_2$) is maintained in the face of reduced cerebral perfusion pressure by increasing oxygen extraction fraction (Powers, 1991). This increases the deoxy:oxyhemoglobin ratio in the vasculature, resulting in a decreased T_2^* signal within penumbra. Increased oxygen delivery during OC will convert deoxyhemoglobin back to oxyhemoglobin, with a resultant increase in T_2^* signal, the magnitude of which should be greatest in regions with greatest oxygen extraction fraction. T_2^* maps can be generated that locate and quantify the percentage change in T_2^* signal throughout the territory of the occluded artery. In addition, the maintenance of this increased signal during the OC and its return back to baseline following OC is consistent with T_2^* signal change, indicating oxygen consumption. This technique may therefore yield information on oxygen metabolism that more closely correlates with positron emission tomography definitions of the penumbra.

In our previous study (Santosh *et al*, 2008), the OC technique applied to a rodent middle cerebral artery occlusion (MCAO) model defined an inner boundary between metabolically inactive ischemic core (no T_2^* signal increase to OC) and metabolically active penumbra (T_2^* signal increase to OC), which overlapped approximately with DWI/PWI mismatch, and correlated with the histological appearances of neuronal integrity. The greater magnitude of T_2^* signal increase in penumbra during OC compared with normal cortex may differentiate between hypoperfused penumbra and benign oligemic tissue on the basis of differences in $CMRO_2$, thereby providing a means of defining the outer boundary of the penumbra.

The aim of this study was to provide further validation for the T_2^* OC MRI technique: first to confirm viability of tissue within regions defined as penumbra using OC. This was achieved by coregistering T_2^* OC maps with corresponding [^{14}C]2-deoxyglucose (2-DG) autoradiograms, which provide information on local cerebral glucose utilization (LCMRglu) as a quantitative representation of metabolic activity. Second, regions of interest (ROIs) identified on 2-DG autoradiograms and MRI scans were investigated to determine the LCMRglu and MRI signatures of different tissue compartments in the ischemic hemisphere.

Materials and methods

Rodent Middle Cerebral Artery Occlusion Surgery

Experiments were performed under license from the UK Home Office and were subject to the Animals (Scientific Procedures) Act, 1986. Male Sprague-Dawley rats (289 ± 13 g, $n = 6$, Harlan, Bicester, UK), fasted overnight, were initially anesthetized with 5% inhaled isoflurane in an induction chamber at room temperature. Following a surgical tracheotomy, animals were artificially ventilated with 2% isoflurane delivered in air, slightly enriched with oxygen (30%) to maintain physiological stability throughout the experiment. Blood gases were sampled at baseline in the 5 minutes before the start of OC, and half way through 100% O_2 inhalation, and maintained within the normal physiological range apart from increased arterial partial pressure of oxygen (PaO_2) during the OC. $PaCO_2$ was maintained between 35 and 45 mm Hg to minimize cerebrovascular reactivity (Table 1). A rectal thermocouple provided continual monitoring of core body temperature, which was maintained at $37^{\circ}C \pm 0.5^{\circ}C$.

Polyethylene catheters (Portex: external diameter 0.96 mm; internal diameter 0.58 mm; 70 cm long) were placed in both femoral arteries, to continuously monitor blood pressure and conduct blood gas analysis, and a femoral vein for 2-DG administration. Middle cerebral artery occlusion was achieved by the intraluminal filament

Table 1 Physiological variables at baseline and during OC

Physiological data (n = *6*)

	Baseline	*During OC*
MABP	82.4 ± 7	91.4 ± 6.7*
$PaCO_2$ (mm Hg)	34.8 ± 7	36.3 ± 8.5
PaO_2 (mm Hg)	85.8 ± 7.4	310.6 ± 84.1**
Blood pH	7.32 ± 0.04	7.32 ± 0.04

MABP, mean arterial blood pressure; OC, oxygen challenge.
Data are expressed as mean ± s.d., $*P < 0.05$ and $**P < 0.0001$, Student's paired *t*-test.

technique (Longa *et al*, 1989), where a 3-0 nylon monofilament with a bulbed tip was introduced through the internal carotid artery and advanced to block the origin of the MCA.

Magnetic Resonance Imaging Scanning

Magnetic resonance imaging data were acquired on a Bruker Biospec 7-T/30-cm system equipped with an inserted gradient coil (121 mm ID, 400 mT/m) and a 72-mm birdcage resonator. After stroke surgery, animals were placed prone in a rat cradle, with the head restrained using ear and tooth bars to limit movement, and a linear surface receiver coil (2 cm diameter) placed above the head of the animal.

T_2 Scanning

A RARE T_2 sequence (effective TE: 46.8 milliseconds, TR: 5,000 milliseconds; in-plane resolution of 97 μm; 30 slices of 0.5 mm thickness) provided the neuroanatomical template for coregistration of T_2^* scans with DWI and PWI scans and 2-DG autoradiograms (Figures 1A and 1B).

T_2^* Scanning

The sequence used to measure T_2^* changes during OC was a single shot, gradient echo (echo planar imaging) sequence. (TE: 20 milliseconds, TR: 10 milliseconds, matrix 96×96, field of view: $25 \times 25\,mm^2$, eight contiguous slices of 1.5 mm thickness, two averages, temporal resolution 20 seconds, 75 repetitions). Two coronal MRI slices, which corresponded to territory supplied by the MCA, were selected for analysis. The paradigm for the T_2^*-weighted OC sequence was 5 minutes breathing air, followed by 5 minutes breathing 100% oxygen, and then 15 minutes breathing air.

Diffusion-Weighted Imaging

DWI was performed to identify ischemically injured tissue (spin echo (echo planar imaging) TE: 43 milliseconds, TR: 4,000.3 milliseconds, in-plane resolution of 260 μm, three directions: *x*, *y*, *z*, *B* values: 0, 1,000 s/mm^2, eight slices of 1.5 mm thickness).

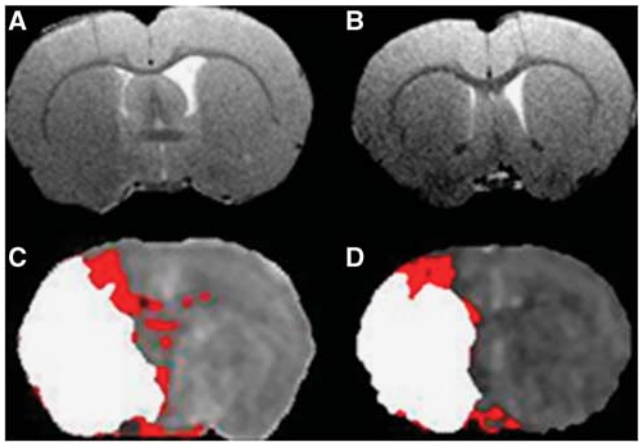

Figure 1 RARE T_2 neuroanatomical templates for caudal (**A**) and rostral (**B**) middle cerebral artery territory slices of interest. Corresponding coregistered perfusion-weighted imaging (PWI) and diffusion-weighted imaging (DWI) threshold images displaying DWI lesion (white) superimposed on perfusion deficit (red), revealing DWI/PWI mismatch areas for caudal (**C**) and rostral (**D**) slices.

Arterial Spin Labeling

Noninvasive quantitative cerebral blood flow (CBF) was performed on two coronal slices within the MCA territory using a form of pseudo-continuous arterial spin labeling (ASL) based on a train of adiabatic inversion pulses (Moffat *et al*, 2005). The sequence uses a spin echo, echo planar imaging module (TE: 20 milliseconds, TR: 7,000 milliseconds, matrix 96×96, field of view: $25 \times 25\,mm^2$, slice thickness 1.5 mm, 16 averages, 4 shots) preceded by 50 hyperbolic secant inversion pulses in a 3-second train.

[^{14}C]2-Deoxyglucose Autoradiography

At the end of the MRI scanning session, animals were quickly removed from the magnet, and a bolus of 2-DG injected intravenously at a steady rate over 30 seconds (125 μCi/kg in 0.6 mL heparinized saline, Perkin-Elmer, Waltham, MA, USA). Plasma glucose and ^{14}C were analyzed from 14 timed arterial blood samples over 45 minutes by glucose oxidase assay and liquid scintillation analysis, respectively. At 45 minutes, animals were rapidly killed by intravenous injection of sodium pentobarbitone and the brains quickly dissected out, frozen (isopentane, −40 °C) and processed for quantitative autoradiography. Coronal cryostat sections (20 μm) were exposed to X-ray film (Kodak Biomax MR film, Eastman Kodak Company, Rochester, NY, USA) for 3 days with a set of ^{14}C standards (Amersham Biosciences, GE Healthcare, Little Chalfont, Buckinghamshire, UK). Autoradiograms were analyzed using a computer digitized image analysis system (MCID v4, Interfocus, Linton, Cambridge, UK).

Quantitative optical density measurements were taken from five ROIs (defined in detail below and shown in Figure 2): (1) ischemic core; (2) penumbra; (3) an

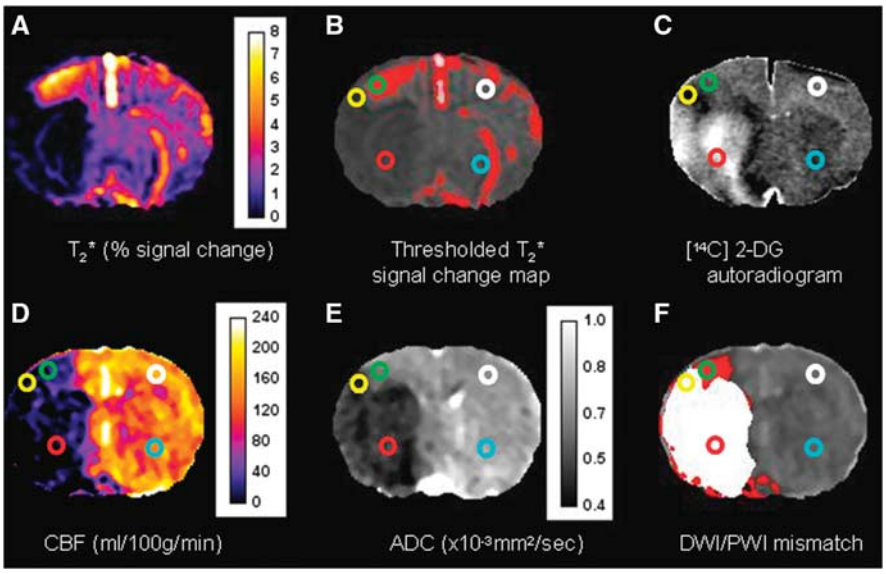

Figure 2 Representative magnetic resonance imaging (MRI) maps and [^{14}C]2-deoxyglucose (2-DG) autoradiograms from the rostral slice in a stroke rat. (**A**) T_2^* Oxygen challenge (OC) percentage signal change map. (**B**) Thresholded T_2^* OC map. (**C**) [^{14}C]2-deoxyglucose autoradiogram. (**D**) Cerebral blood flow (CBF) map (mL per 100 g per minute). (**E**) Apparent diffusion coefficient (ADC) map ($\times 10^{-3}$ mm^2/s). (**F**) Diffusion-weighted imaging/perfusion-weighted imaging (DWI/PWI) overlay (mismatch tissue is shown in red). Regions of interest (ROIs) were defined as follows: Green ROI: penumbra—the thresholded region displaying the greatest T_2^* percentage signal change excluding veins and ventricles (**B**). Yellow ROI: hyperglycolytic region—identified by the dark band within the ipsilateral cortex on the 2-DG autoradiogram (**C**). Red ROI: ischemic core—within the ADC-derived lesion in the caudate nucleus (**E**). White ROI: contralateral cortex—homotopic to the penumbra ROI. Sky Blue ROI: contralateral caudate nucleus—homotopic to the ischemic core ROI.

intermediate region of increased glucose utilization at the boundary of the ischemic core (see Figure 2C); (4) and (5) contralateral regions homotopic to the penumbra and ischemic core, respectively. Optical density values were converted into ^{14}C tissue concentrations using the calibration curve derived from the set of ^{14}C standards. The ^{14}C tissue concentrations along with the plasma glucose and ^{14}C plasma concentrations were used to calculate LCMRglu (μmol per 100 g per minute) in ROIs using the operational equation of Sokoloff *et al* (1977).

Glucose utilization for each ROI was generated from 10 autoradiographic images covering the rostro-caudal extent of each MRI slice (1.5 mm) to accurately equate T_2^* signal change maps with glucose utilization.

Defining the Ischemic Penumbra with T_2^* Oxygen Challenge

The time course and size of the T_2^* signal change was analyzed within ROIs (see Figure 3). T_2^* percentage signal change was calculated from time course graphs, where the average baseline signal was subtracted from the peak signal during OC. This value was then divided by the average baseline signal and multiplied by 100. T_2^* OC percentage signal change maps were generated using Image J software (http://rsb.info.nih.gov/ij/).

Penumbral tissue was defined using a threshold based on the empirical rule: the mean plus 2 s.d. of the T_2^* value of the contralateral hemisphere, excluding the ventricles (see Figure 2B).

Defining the Ischemic Penumbra with DWI/PWI Mismatch

Diffusion-weighted imaging and PWI (using ASL) were used to define mismatch before the T_2^* OC protocol and data were analyzed on two selected coronal slices within the MCA territory (Figure 1). Quantitative ADC_{av} maps, in units of square millimeters per second, were calculated using the Stejskal–Tanner equation (Stejskal and Tanner, 1965). Apparent diffusion coefficient maps and CBF maps were generated using Image J software. A 16.5% reduction of mean contralateral ADC was used to determine ischemic lesion volume, which has been shown to match closely the final infarct size following permanent MCAO in Sprague-Dawley rats (Lo *et al*, 1997). Perfusion-weighted imaging was performed on the fifth and sixth coronal slices within core MCA territory and the perfusion deficit area was calculated based on a 57% reduction of mean contralateral CBF (Meng *et al*, 2004). ADC and CBF maps were overlaid to identify the DWI/PWI mismatch area defined as the difference between the perfusion deficit and the ADC lesion area on the corresponding slice. For analysis, the data for the rostral and caudal slices were combined.

Volumetric Analysis of Penumbra, Hypo- and Hyperglycemic Tissues

Volumetric analysis of penumbra (in terms of mismatch and the T_2^* OC), ADC-defined lesion, perfusion deficit and hypo- and hyperglycemic tissue on 2-deoxyglucose auto-

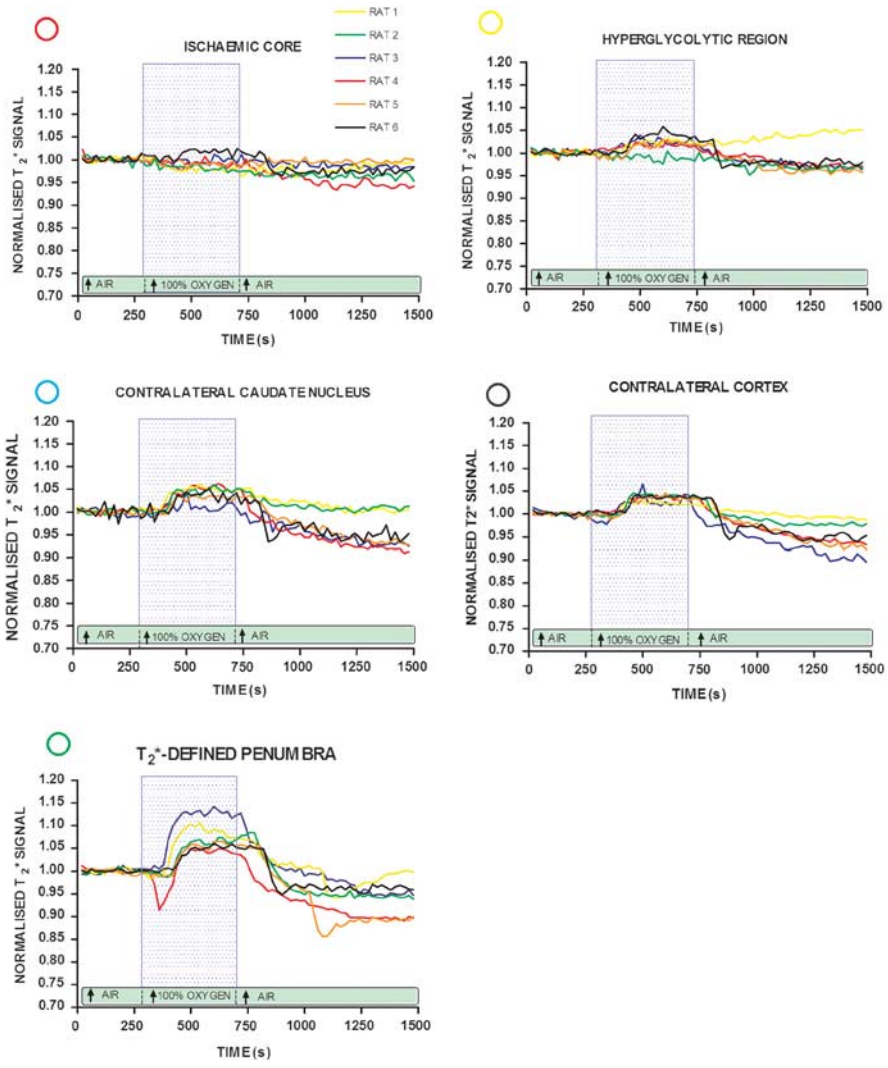

Figure 3 Echo planar imaging (EPI) T_2^* oxygen challenge (OC) signal time course: time course T_2^* signal change during OC in: apparent diffusion coefficient (ADC)-derived ischemic core (red circle); cortical hyperglycolytic region from 2-deoxyglucose autoradiogram (yellow circle); a region corresponding to the greatest T_2^* percentage signal change increase adjacent to hyperglycolytic band (green circle); corresponding regions on: the contralateral cortex (black circle) and caudate nucleus (sky blue circle). Each line represents data from a single animal. Within each animal, all data were normalized to the average signal over the 5-minute before OC. Blue box represents the period of 100% oxygen inhalation.

radiograms were performed and data expressed as the mean volume over the rostro-caudal extent of the ASL scans. For 2-deoxyglucose autoradiograms, images were analyzed to cover the same rostro-caudal extent as the MR images, and were thresholded to determine the region of severely reduced glucose use (glucose values below 10 μmol per 100 g per minute) and the hyperglycolytic band (tissue with glucose values above 60 μmol per 100 g per minute).

Regions of Interest

Circular ROIs were selected according to specific features on the images (Figure 2). To ensure placement solely within the areas of interest and uniformity in ROI size, ROIs were chosen manually (spanning 80 pixels). The researcher responsible for ROI placement was blinded to the autoradiograph data during MRI ROI placement and *vice versa*. Magnetic resonance imaging-based ROIs were defined and placed within (1) ischemic core in caudate nucleus within the thresholded ADC lesion (Figure 2E, red); (2) its mirror contralateral region (sky blue), manually designated by researcher; (3) penumbra as defined by thresholded T_2^* percentage signal change (Figure 2B, green); (4) equivalent contralateral cortex (white), and (5) a cortical hyperglycolytic region selected from the 2-DG autoradiogram (Figure 2C, yellow).

Coregistration and Regions of Interest Analysis

The processed data from the T_2^* OC, 2-DG, thresholded ADC and CBF maps, were coregistered to: (1) generate ROI data and (2) identify the location of the DWI/PWI mismatch

(Figures 1C and 1D). Linear coregistration was first performed using Analyze (AnalyzeDirect, Inc. Overland Park, KS, USA) and then DWI, ASL, T_2^*- and 2-DG images were warped to their corresponding RARE T_2 slices using AIR 5.2.6 (Automated Image Registration (Woods *et al*, 1998)).

Statistical Analysis

All data are presented as mean ± s.d. Data were normally distributed, and as such, physiological variables at baseline (pre-OC) and during OC were analyzed by Student's paired *t*-test. T_2^* signal, ADC, CBF, and LCMRglu values in different ROIs were analyzed by one-way analysis of variance followed by Student's paired *t*-test with a Bonferroni correction for multiple comparisons. A paired *t*-test was used to analyze the temporal evolution of the ADC-derived lesion volume. All data were tested to confirm normal distribution using the D'Agostino and Pearson normality test.

Results

Physiological Variables

Mean time to commence OC was 147 ± 32 minutes after MCAO. Physiological variables were recorded immediately before and during OC (Table 1). PaO_2 increased significantly (262%, $P<0.0001$) as expected during OC, $PaCO_2$ did not change and mean arterial blood pressure increased significantly (11%, $P<0.05$). The mean plasma glucose before scanning was 9.8 ± 2.7 mmol/L.

T_2^* Percentage Signal Change to Oxygen Challenge

T_2^* percentage signal change during OC was measured over two coronal slices. Thresholded T_2^* maps revealed a region of increased signal, which corresponded approximately with the DWI/PWI mismatch (Figures 2B and 2F). Examining the individual T_2^* time course data (Figure 3), T_2^* signal increase in this penumbral ROI was 9.2% ± 3.9%, significantly greater than in the contralateral ROI (2.76% ± 0.3%, $P<0.001$; Figure 4). In ischemic core, mean T_2^* signal during OC was reduced (−0.49% ± 1.6%) compared with the contralateral caudate nucleus ROI (3.56% ± 0.94%, $P<0.01$). In the hyperglycolytic ROI, there was a small T_2^* signal increase of 1.4% ± 0.6%, significantly smaller than the response in the contralateral cortex ($P<0.05$) and penumbral ROI ($P<0.001$).

Glucose Use Values in Regions of Interest

[^{14}C]2-deoxyglucose autoradiography confirmed glucose use within the T_2^* OC-defined penumbra, which was not significantly different from the contralateral ROI (22.67 ± 2.1 μmol per 100 g per minute compared with 20.1 ± 2.3 μmol per 100 g per minute; Figure 5). Glucose use was below the limit of detection in ischemic core (Figures 2C and 5) and was markedly

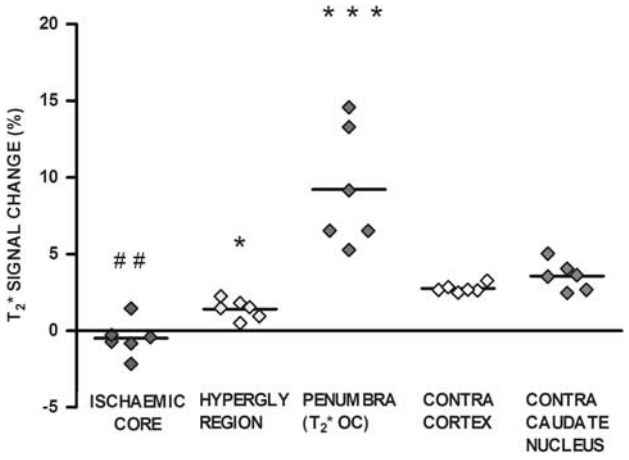

Figure 4 T_2^* percentage signal change from baseline in regions of interest (ROIs). Individual animal data with horizontal lines representing means. $^{***}P<0.001$ and $^{*}P<0.05$ relative to contralateral cortex ROI. $^{\#\#}P<0.01$ relative to contralateral caudate nucleus.

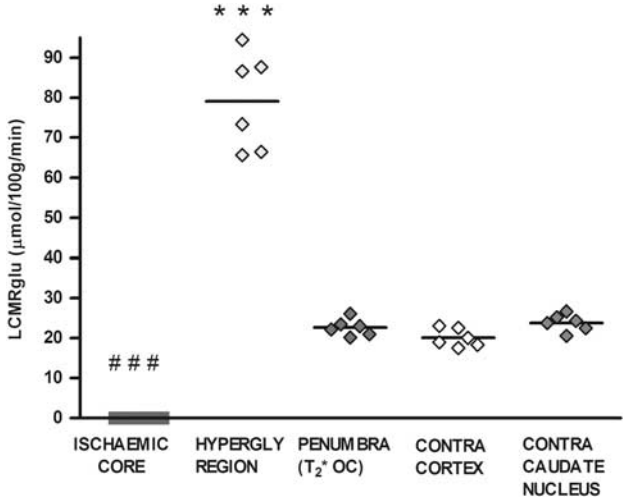

Figure 5 Local cerebral glucose utilization (LCMRglu) in regions of interest (ROIs). Individual animal data with horizontal lines representing means. $^{***}P<0.001$ relative to contralateral cortex. $^{\#\#\#}P<0.001$ relative to contralateral caudate nucleus.

increased in the hyperglycolytic ROI (79.7 ± 12 μmol per 100 g per minute, compared with contralateral cortex 20.1 ± 2.3 μmol per 100 g per minute, $P<0.001$). The hyperglycolytic ROI (279% increase in LCMRglu) occurred within the boundary of the ADC lesion. It displayed a small increase in T_2^* signal to OC, which was significantly smaller ($P<0.05$) than the T_2^* increase in contralateral cortex (Figure 4).

Absolute glucose utilization values were low compared with most values from the literature, which are generated from conscious animals. To confirm the validity of our 2-DG technique, in an additional animal, anesthesia was withdrawn following MRI scanning and 2-DG autoradiography performed 2 hours later when the animal was fully conscious. Glucose use values were similar to

reported values, and proportionally higher in each ROI, when compared with anesthetized animals: contralateral cortex 41.67 μmol per 100 g per minute; contralateral caudate nucleus 46.7 μmol per 100 g per minute; penumbra, 69 μmol per 100 g per minute (62% increase); hyperglycolytic ROI, 91 μmol per 100 g per minute (122% increase); ischemic core, 1.43 μmol per 100 g per minute (97% decrease relative to contralateral caudate nucleus). Therefore, the low glucose utilization values in the MRI study were most likely due to the level and duration of anesthesia (see Supplementary Material).

To dismiss the possibility that the presence of the hyperglycolytic band may be a confound of O_2 administration, an additional rat underwent MCAO, and when fully conscious 2-DG autoradiography was performed without OC. The hyperglycolytic band was present, suggesting the OC *per se* was not responsible for generating hyperglycolytic tissue.

Severity of Ischemia and Tissue Viability

On quantitative CBF maps (Figure 2D), contralateral cortex and caudate nucleus ROIs had mean CBF values of 185 ± 45 and 165 ± 31 mL per 100 g per minute, respectively. Cerebral blood flow within ischemic core, hyperglycolytic, and penumbra ROIs was significantly reduced (7.9 ± 4.7, 21 ± 0.2, and 37 ± 66 mL per 100 g per minute, respectively, all $P < 0.001$) relative to the equivalent contralateral ROI (Figure 6A).

On ADC maps (Figure 2E), ROIs in contralateral cortex and caudate nucleus had a mean ADC of 0.73 ± 0.06 and $0.74 \pm 0.02 \times 10^{-3}$ mm^2/s, respectively (Figure 6B). Apparent diffusion coefficient values were significantly reduced in ischemic core and hyperglycolytic ROIs (0.47 ± 0.04 and $0.51 \pm 0.08 \times 10^{-3}$ mm^2/s, respectively, $P < 0.001$), while in the T_2^* OC-defined penumbral ROI, mean ADC value ($0.71 \pm 0.04 \times 10^{-3}$ mm^2/s) was not significantly reduced compared with contralateral cortex ($P > 0.05$; Figure 6B).

Penumbra Defined by Diffusion-Weighted Imaging/ Perfusion-Weighted Imaging Mismatch

For comparison, penumbra, as defined by DWI/PWI mismatch was mapped over two coronal slices from the coregistered ADC and ASL scans (Figures 1C and 1D and 2F).

Evolution of Apparent Diffusion Coefficient-Derived Lesion Volume

Diffusion-weighted imaging scans generated at the start and conclusion of the MRI scanning session provided information on the evolution of ischemic injury over time. A significant increase in the ADC-derived lesion volume (106 ± 66 mm^3 at 52 ± 11 minutes compared with 185 ± 130 mm^3 at 106 ± 8 minutes after stroke, $P < 0.05$) highlighted the progression of damage in the acute stroke period and the concomitant loss of penumbral tissue.

Volumetric Analysis of Penumbra, Hypo- and Hyperglycemic Tissues

The volume of perfusion deficit determined at 76.4 ± 13.2 minutes after stroke, was 103.1 ± 21 mm^3, the ADC lesion volume, determined at 106 ± 8 minutes after stroke was 80.7 ± 30 mm^3, generating a DWI/PWI mismatch volume of 22.3 ± 19 mm^3. The thresholded T_2^* OC-defined penumbra, determined at 147 ± 32 minutes, was 15 ± 9 mm^3. Mismatch- and T_2^* OC-defined penumbral volumes were $\sim$28% and 19% of the volume of the ADC-defined ischemic core, respectively. The volume of tissue with severely reduced glucose use in ischemic core was 52.8 ± 18 mm^3 and the volume of the hyperglycolytic band was 21.1 ± 16 mm^3.

Discussion

We previously described the OC MRI technique in a focal cerebral ischemia model and compared it with

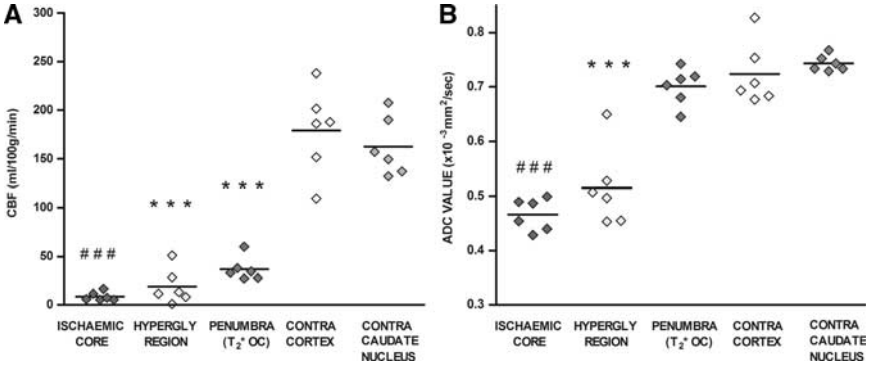

Figure 6 Cerebral blood flow (CBF) (**A**) and apparent diffusion coefficient (ADC) (**B**) in regions of interest (ROIs). Individual animal data with horizontal lines representing means. ***, ###($P < 0.001$) relative to contralateral cortex and contralateral caudate nucleus, respectively.

DWI/PWI mismatch and histologically defined neuronal morphology (Santosh *et al*, 2008). We have also demonstrated feasibility of the technique in clinical use in acute stroke (Dani *et al*, 2010). The current study provides evidence of ongoing metabolism in T_2^* OC-defined penumbra and provides more direct validation for the technique. In addition, coregistration of 2-DG autoradiography with MRI has provided detailed information on the adjacent tissue compartments within the ischemic hemisphere, which show markedly different levels of glucose metabolism. We propose that the T_2^* OC technique indirectly identifies penumbra from its higher oxygen extraction fraction, which influences deoxy/oxyhemoglobin ratios and T_2^* signal. However, we acknowledge that other factors may give rise to an increase in T_2^* signal in the penumbra. For example, an increased cerebral blood volume in penumbral tissue may increase deoxyhemoglobin in this region, thus magnifying the T_2^* response.

MRI-defined DWI–PWI mismatch identifies penumbra in a similar, but not exact, neuroanatomical location (Figure 2). However, the underlying assumptions are undermined by reversibility of the DWI lesion with reperfusion, uncertainty over relevant perfusion thresholds, and the variable metabolic state of DWI lesion voxels. Information on metabolic state should improve penumbral definition. Blood oxygen level-dependent MRI offers information on oxygen consumption and delivery (Baird and Warach, 1999; Kavec *et al*, 2001), but static T_2^*-weighted MRI under normoxic conditions has not adequately delineated penumbra in ischemic stroke patients (Tamura *et al*, 2002; Grohn and Kauppinen, 2001), possibly because deoxyhemoglobin is not rapidly cleared in ischemic conditions (Giesler *et al*, 2006). We hypothesized that mapping dynamic changes in T_2^* in response to OC should improve discrimination between penumbra and surrounding tissue compartments (Santosh *et al*, 2008).

Our results show a region of significant T_2^* increase during OC localized to a cortical boundary zone between the MCA and anterior cerebral artery territories, which overlaps with the DWI/PWI mismatch area. This region displayed metabolism on coregistered autoradiograms not significantly different from contralateral normal tissue, and significantly greater than infarct core, which is consistent with previous 2-DG studies in acute focal ischemia (Belayev *et al*, 1997; Tohyama *et al*, 1998).

A smaller T_2^* signal increase to OC, compared with penumbral tissue, would also be expected in normal metabolizing tissue (as shown in Santosh *et al*, 2008) and in all six animals, the hemisphere contralateral to MCAO showed measurable increases in T_2^* signal intensity during OC (Figures 3 and 4). By coregistering thresholded T_2^* maps with glucose use autoradiograms, a metabolic signature of normal tissue was generated to allow comparison with the ischemic hemisphere. Our MR findings were consistent with the previous study (Santosh *et al*, 2008), in which the ischemic core, defined by ADC, was notable as a region with negligible T_2^* signal change. It registered undetectable glucose use values, thus confirming metabolic inactivity in this tissue compartment where $CMRO_2$ and oxygen extraction fraction would be expected to be markedly reduced or absent.

An intermediate tissue compartment, identified as hyperglycolytic on autoradiograms, displayed a small (subthreshold) T_2^* signal change and lay inside the boundary of the ADC abnormality (Figures 2, 3, and 5). This may point to residual oxygen utilization on the border of the ADC abnormality (Figure 4), in tissue with ADC and CBF values intermediate between the ischemic core and T_2^*-defined penumbra (Figures 6A and 6B). The presence of hyperglycolysis within the ADC lesion suggests the tissue is still metabolically active, and may not be irreversibly injured at this time point. This region may therefore be critically injured and employing anaerobic glycolysis (Nedergaard and Astrup, 1986), which cannot sustain viability. As some oxygen is being extracted from the blood, this suggests some oxidative metabolism persists but may indicate tissue destined for rapid, irreversible damage. This supports recent blood oxygen level-dependent MR studies that propose the ADC lesion may not only incorporate tissue that is destined to die, but also severely injured, still viable tissue (Kidwell *et al*, 2002). A number of studies have reported reversibility of the ADC lesion following reperfusion (Mintorovitch *et al*, 1991; Minematsu *et al*, 1992; Kidwell *et al*, 2000). Hypermetabolic tissue displaying a small T_2^* percentage signal change may therefore indicate an intermediate compartment of the ischemic penumbra situated within both the ADC abnormality and the perfusion deficit, whose fate may be being determined by secondary insults after stroke, such as preterminal spreading depolarizations, which may exhaust ATP levels in vulnerable cells.

Limitations of the DWI/PWI Mismatch Technique

Despite its limitations, the DWI/PWI mismatch model provides information on location and severity of ischemia (derived from PWI), tissue viability status (ADC values derived from DWI), and therefore approximate location and size of penumbra. Perfusion-weighted imaging and DWI scans were therefore included in the scanning routine for comparison with T_2^* OC identification of penumbra. A number of studies have shown that differentiation between viable and nonviable tissue is difficult, using the diffusion abnormality (Kidwell *et al*, 2000; Fiehler *et al*, 2002), which correlates poorly with final infarct (Li *et al*, 1999). As mentioned above, DWI lesions may be recoverable following prompt reperfusion in animal models and humans, and may not be destined for infarction (Schlaug *et al*, 1997; Mintorovitch *et al*, 1991; Kidwell *et al*, 2000). Additionally, the

perfusion deficit may incorporate tissue with benign oligemia (destined to survive) even when optimal MRI thresholds (themselves as yet incompletely defined) are applied (Butcher *et al*, 2005). As such, the inner and outer margins of the penumbra may not be adequately delineated using the mismatch technique, which has been shown to frequently overestimate the final lesion size (Kucinski *et al*, 2005).

Limitations of the Study

The [^{14}C]2-DG method may not have accurately defined LCMRglu because the increase in radioactivity registered may either be a result of real glucose consumption or a methodological artifact from an increase in the lumped constant. In normal conditions, the lumped constant used for the 2-DG technique is stable over a large spectrum of plasma glucose concentrations (Sokoloff *et al*, 1977). With reduced glucose supply—such as during ischemia—the lumped constant may increase considerably (Suda *et al*, 1990; Vannucci *et al*, 1989; Gilland and Hagberg, 1996). As there is reduced glucose availability, the glucose distribution volume decreases and the lumped constant increases because 2-DG is the preferred sugar for phosphorylation by hexokinase. As such, local values of the lumped constant should be estimated, which may be derived by measuring the brain uptake of methlyglucose (Dienel *et al*, 1991; Gjedde *et al*, 1985). Another limitation is the lack of a gold standard or independent identification method for penumbra to compare T_2^* OC with.

Summary

The T_2^* OC technique represents a clinically translatable method of yielding metabolic information from the ischemic brain that may improve delineation of penumbral tissue after acute ischemic stroke. By exploiting the different magnetic properties of oxy- and deoxyhemoglobin, the dynamic response to oxygen administration may detect tissue capacity for oxygen utilization and define the ischemic penumbra on the basis of oxygen extraction and metabolism. This study therefore supports the utility of the OC technique to provide information on oxygen metabolism and tissue viability following stroke.

Disclosure/conflict of interest

The authors declare no conflict of interest.

References

Albers GW, Thijs VN, Wechsler L, Kemp S, Schlaug G, Skalabrin E, Bammer R, Kakuda W, Lansberg MG, Shuaib A, Coplin W, Hamilton S, Moseley M, Marks MP (2006) Diffusion and perfusion imaging evaluation for understanding stroke evolution: the DEFUSE study. *Ann Neurol* 60:508–17

Baird AE, Warach S (1999) Imaging developing brain infarction. *Curr Opin Neurol* 12:65–71

Barber PA, Zhang J, Demchuk M, Hill MD, Buchan AM (2001) Why are stroke patients excluded from TPA therapy? An analysis of patient ineligibility. *Neurology* 56:1015–20

Belayev L, Zhao W, Busto R, Ginsberg MD (1997) Transient middle cerebral artery occlusion by intraluminal suture: I. Three-dimensional autoradiographic image-analysis of local cerebral glucose metabolism-blood flow interrelationships during ischemia and early recirculation. *J Cereb Blood Flow Metab* 17:1266–80

Butcher KS, Parsons M, MacGregor L, Barber PA, Chalk J, Bladin C, Levi C, Kimber T, Schultz D, Fink J, Tress B, Donnan G, Davis S (2005) Refining the perfusion–diffusion mismatch hypothesis. *Stroke* 36:1153–9

Dani KA, Santosh C, Brennan D, McCabe C, Holmes WM, Condon B, Hadley DM, Macrae IM, Shaw M, Muir KW (2010) T2* weighted magnetic resonance imaging with hyperoxia in acute ischemic stroke. *Ann Neurol* 68:37–47

Dienel GA, Cruz NF, Mori K, Holden JE, Sokoloff L (1991) Direct measurement of the lambda of the lumped constant of the deoxyglucose method in rat brain: determination of lambda and lumped constant from tissue glucose concentration or equilibrium brain/plasma distribution ratio for methylglucose. *J Cereb Blood Flow Metab* 11:25–34

Donnan GA, Fisher M, Macleod M, Davis SM (2008) Stroke. *Lancet* 371:1612–23

Fiehler J, Foth M, Kucinski T, Knab R, von Bezold M, Weiller C, Zeumer H, Röther J (2002) Severe ADC decreases do not predict irreversible tissue damage in humans. *Stroke* 33:79–86

Geisler BS, Brandhoff F, Fiehler J, Saager C, Speck O, Rother J, Zeumer H, Kuncinski T (2006) Blood oxygen level-dependent MRI allows metabolic description of tissue at risk in acute stroke patients. *Stroke* 37:1778–84

Gilland E, Hagberg H (1996) NMDA receptor-dependent increase of cerebral glucose utilization after hypoxia-ischemia in the immature rat. *J Cereb Blood Flow Metab* 16:1005–13

Gjedde A, Wienhard K, Heiss WD, Kloster G, Diemer NH, Herholz K, Pawlik GJ (1985) Comparative regional analysis of 2-fluorodeoxyglucose and methylglucose uptake in brain of four stroke patients. With special reference to the regional estimation of the lumped constant. *J Cereb Blood Flow Metab* 5:163–78

Grohn OH, Kauppinen RA (2001) Assessment of brain tissue viability in acute ischemic stroke by BOLD MRI. *NMR Biomed* 14:432–40

Guadagno JV, Warburton EA, Aigbirhio FI, Smielewski P, Fryer TD, Harding S, Price CJ, Gillard JH, Carpenter TA, Baron JC (2004) Does the acute diffusion-weighted imaging represent penumbra as well as core? A combined quantitative PET/MRI voxel-based study. *J Cereb Blood Flow Metab* 24:1249–54

Hacke W, Albers G, Al-Rawi Y, Bogousslavsky J, Davalos A, Eliasziw M, Fischer M, Furlan A, Kaste M, Lees KR, Soehngen M, Warach S; DIAS Study Group (2005) The Desmoteplase in Acute Ischemic Stroke Trial (DIAS): a phase II MRI-based 9-hour window acute stroke thrombolysis trial with intravenous desmoteplase. *Stroke* 36:66–73

Hacke W, Kaste M, Fieschi C, von Kummer R, Davalos A, Meier D, Larrue V, Bluhmki E, Davis S, Donnan G, Schneider D, Diez-Tejedor E, Trouillas P (1998) Randomised double-blind placebo controlled trial of thrombolytic therapy with intravenous alteplase in acute ischaemic stroke (ECASS II). Second European-Australasian Acute Stroke Study Investigators. *Lancet* 352:1245–51

Kahn JH, Viereck J, Kase C, Jeerakathil T, Romero R, Mehta SD, Kociol R, Babikian V (2005) The use of intravenous recombinant tissue plasminogen activator in acute ischemic stroke. *J Emerg Med* 29:273–7

Katzan IL, Hammer MD, Hixson ED, Furlan AJ, Abou-Chebl A, Nadzam DM, Cleveland Clinic Health System Stroke Quality Improvement Team (2004) Utilization of intravenous tissue plasminogen activator for acute ischemic stroke. *Arch Neurol* 61:346–50

Kavec M, Gröhn OHJ, Kettunen MI, Silvennoinen MJ, Penttonen M, Kauppinen RA (2001) Use of spin echo T2 BOLD in assessment of misery perfusion at 1.5 T. *MAGMA* 12:32–9

Kidwell CS, Liebeskind DS, Starkman S, Saver JL (2001) Trends in acute ischemic stroke trials through the 20th century. *Stroke* 32:1349–59

Kidwell CS, Saver JL, Mattiello J, Starkman S, Vinuela F, Duckwiler D, Gobin YP, Jahan R, Vespa P, Kalafut M, Alger JR (2000) Thrombolytic reversal of acute human cerebral ischemic injury shown by diffusion/perfusion magnetic resonance imaging. *Ann Neurol* 47: 462–9

Kidwell CS, Saver JL, Starkman S, Duckwiler G, Jahan R, Vespa P, Villablanca JP, Liebeskind DS, Gobin YP, Vinuela F, Alger JR (2002) Late secondary ischemic injury in patients receiving intraarterial thrombolysis. *Ann Neurol* 52:698–703

Kucinski T, Naumann D, Knab R, Schoder V, Wegener S, Fiehler J, Majumder A, Röther J, Zeumer H (2005) Tissue at risk is overestimated in perfusion-weighted imaging: MR imaging in acute stroke patients without vessel recanalization. *Am J Neuroradiol* 26:815–9

Li F, Han S, Tatlisumak T, Liu KF, Garcia JH, Sotak CH, Fisher M (1999) Reversal of acute apparent diffusion coefficient abnormalities and delayed neuronal death following transient focal cerebral ischemia in rats. *Ann Neurol* 46:333–42

Lo EH, Pierce AR, Mandeville JB, Rosen BR (1997) Neuroprotection with NBQX in rat focal cerebral ischemia. Effects on ADC probability distribution functions and diffusion–perfusion relationships. *Stroke* 28:439–47

Longa EZ, Weinstein PR, Carlson S, Cummins R (1989) Reversible middle cerebral artery occlusion without craniectomy in rats. *Stroke* 20:84–91

Meng X, Fisher M, Shen Q, Sotak CH, Duong TQ (2004) Characterizing the diffusion/perfusion mismatch in experimental focal cerebral ischemia. *Ann Neurol* 55:207–12

Minematsu K, Li L, Sotak CH, Davis MA, Fisher M (1992) Reversible focal ischemic injury demonstrated by diffusion-weighted magnetic resonance imaging in rats. *Stroke* 23:1304–10

Mintorovitch J, Moseley ME, Chileuitt L, Shimizu H, Cohen Y, Weinstein PR (1991) Comparison of diffusion- and T_2-weighted MRI for the early detection of cerebral ischemia and reperfusion in rats. *Magn Reson Med* 18:39–50

Moffat BA, Chenevert TL, Hall DE, Rehemtulla A, Ross BD (2005) Continuous arterial spin labeling using a train of adiabatic inversion pulses. *J Magn Reson Imaging* 21:290–6

Muir KW (2002) Heterogeneity of stroke pathophysiology and neuroprotective clinical trial design. *Stroke* 33:1545–50

Nedergaard M, Astrup J (1986) Infarct rim: effect of hyperglycemia on direct current potential and [14C] 2-deoxyglucose phosphorylation. *J Cereb Blood Flow Metab* 6:607–15

Powers WJ (1991) Cerebral hemodynamics in ischemic cerebrovascular disease. *Ann Neurol* 29:231–40

Santosh C, Brennan D, McCabe C, Macrae IM, Holmes WM, Graham DI, Gallagher L, Condon B, Hadley DM, Muir KW, Gsell W (2008) Potential use of oxygen as a metabolic biosensor in combination with T2(*)-weighted MRI to define the ischemic penumbra. *J Cereb Blood Flow Metab* 28:1742–53

Schellinger PD, Fiebach JB, Hacke W (2003) Imaging-based decision making in thrombolytic therapy for ischemic stroke. *Stroke* 34:575–83

Schlaug G, Siewert B, Benfield A, Edelman RR, Warach S (1997) Time course of the apparent diffusion coefficient (ADC) abnormality in human stroke. *Neurology* 49: 113–9

Sokoloff L, Reivich M, Kennedy C, Des Rosiers MH, Patlak CS, Pettigrew KD, Sakurada O, Shinohara M (1977) The [^{14}C]deoxyglucose method for the measurement of local cerebral glucose utilisation: theory, procedure and normal values in the conscious and anaesthetised albino rat. *J Neurochem* 28:897–916

Stejskal EO, Tanner JE (1965) Spin diffusion measurements: spin echoes in the presence of a time-dependent field gradient. *J Chem Phys* 42:288–92

Suda S, Shinohara M, Miyaoka M, Lucignani G, Kennedy C, Sokoloff L (1990) The lumped constant of the deoxyglucose method in hypoglycemia: effects of moderate hypoglycemia on local cerebral glucose utilization in the rat. *J Cereb Blood Flow Metab* 10:499–509

Tamura H, Hatazawa J, Toyoshima H, Shimosegawa E, Okudera T (2002) Detection of deoxygenation-related signal change in acute ischemic stroke patients by T2*-weighted magnetic resonance imaging. *Stroke* 33:967

Tohyama Y, Sako K, Yonemasu Y (1998) Hypothermia attenuates hyperglycolysis in the periphery of ischemic core in rat brain. *Exp Brain Res* 122:333–8

Uematsu H, Takahashi M, Hatabu H, Chin C, Werli S, Werli F, Asakura T (2007) Changes in T1 and T2 observed in brain magnetic resonance imaging with delivery of high concentrations of oxygen. *J Comput Assist Tomogr* 31: 662–5

Vannucci RC, Christensen MA, Stein DT (1989) Regional cerebral glucose utilization in the immature rat: effect of hypoxia-ischemia. *Pediatr Res* 26:208–14

Wardlaw JM, Sandercock PAG, Murray M (2009) Should more patients with acute ischaemic stroke receive thrombolytic treatment? *BMJ* 339:b4584

Woods RP, Grafton ST, Holmes CJ, Cherry SR, Mazziotta JC (1998) Automated image registration: I. General methods and intrasubject, intramodality validation. *Journal of Computer Assisted Tomography* 22:139–52

Supplementary Information accompanies the paper on the Journal of Cerebral Blood Flow & Metabolism website (http://www.nature.com/jcbfm)